Nonlinear Emission of Molecular Ensembles Strongly Coupled to Plasmonic Lattices with Structural Imperfections

Mohammad Ramezani, Quynh Le-Van, and Alexei Halpin
Department of Applied Physics, Institute for Photonic Integration, Eindhoven University of Technology, P.O. Box 513, 5600 MB, Eindhoven, Netherlands

Jaime Gómez Rivas*
Department of Applied Physics, Institute for Photonic Integration, Eindhoven University of Technology, P.O. Box 513, 5600 MB, Eindhoven, Netherlands
Dutch Institute For Fundamental Energy Research (DIFFER), 5612 AJ, Eindhoven, Netherlands

(Received 21 March 2018; published 14 December 2018)

We demonstrate nonlinear emission from molecular layers strongly coupled to extended light fields in arrays of plasmonic nanoparticles in the presence of structural imperfections. Hybrid light-matter states, known as plasmon-exciton polaritons (PEPs), are formed by the strong coupling of Frenkel excitons in molecules to surface lattice resonances. These resonances result from the radiative coupling of localized surface plasmon polaritons in silver nanoparticles enhanced by diffraction on the array. By designing arrays with different lattice constants, we show that the nonlinear emission frequency is solely determined by the relaxation of exciton polaritons through vibrational quanta in the molecules. We also observe long-range spatial coherence in the samples, which supports the explanation in terms of a nonlinear collective emission of strongly coupled PEPs. In contrast to recent observations of exciton-polariton lasing and condensation in organic systems, photonic modes play a minor role at the emission frequency in our system, and this emission has an undefined momentum because of the structural imperfections. This remarkable result reveals the rich and distinct physics of strongly coupled organic molecules to photonic cavities.

DOI: 10.1103/PhysRevLett.121.243904

Exploring the physics of exciton polaritons, i.e., quasiparticles formed by the strong coupling of light and matter, has been the motivation of many experimental and theoretical works [1]. Room-temperature realizations of strong light-matter coupling have been made possible by combining organic materials and nanophotonic structures [2,3]. In line with previous studies on exciton polaritons in inorganic microcavities at low temperatures, organic exciton polaritons have been shown to exhibit nonlinearities such as optically parametric oscillation [4], polariton lasing [5–7], condensation [8–10], and superfluidity [11].

Coherent emission phenomena, such as exciton-polariton lasing using organic molecules, shares many similarities with its inorganic counterparts at low temperatures. However, there are fundamental differences that distinguish the two phenomena [12]. Unlike the mobile and spatially extended Wannier-Mott excitons found in inorganic semiconductors, Frenkel excitons in organic materials tend to be highly localized to single or few molecules. At low temperatures and in inorganic materials, the dominant relaxation channels leading to polariton lasing or nonequilibrium exciton-polariton condensation are polariton-polariton and polariton-exciton scattering [1], mediated by Coulomb interactions between spatially extended excitons. In contrast, such interactions in organic molecules tend to be weak due to the localized nature of Frenkel excitons. However, an additional relaxation channel exists through intramolecular phonons and vibronic coupling [5,13–15]. In this case, high-frequency Franck-Condon active vibrational modes act to resonantly populate lower-energy polariton states, eventually leading to condensation at a faster rate than that dictated by thermalization through numerous weak scattering events [7,14–16].

In this Letter we use arrays of plasmonic nanoparticles supporting collective modes, known as surface lattice resonances (SLRs), to strongly couple them to the electronic transition of organic molecules in the vicinity of the array with structural imperfections and demonstrate the coherent nonlinear emission. Unlike microcavities, the lattice of plasmonic nanoparticles can be considered as an *open cavity*; i.e., the sample is transparent for most of the energies and momenta except at resonances, and we can directly access the energy and the momentum of the exciton polaritons after the scattering process. This characteristic enables us to observe a transition from spontaneous emission to coherent nonlinear emission of molecules strongly coupled to SLRs. Surprisingly, the emission frequency is solely determined by the relaxation of exciton polaritons through vibrations in the individual molecules collectively coupled to the SLRs, and SLRs do

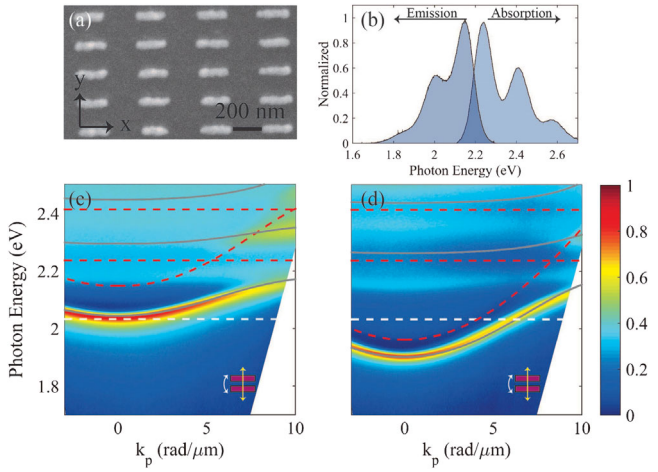

FIG. 1. (a) SEM image of a silver array fabricated on a glass substrate. (b) Normalized absorption and emission spectra of the dye molecules. Measurements of extinction for the array with pitch sizes of (c) 380 nm and (d) 420 nm. The insets indicate the orientation of the array and its rotation direction (white arrow). The yellow arrow represents the polarization of the incident white light. The white dashed line at 2.035 eV shows the energy of the nonlinear emission (See Fig. S5 in the Supplemental Material [17]). The red dashed curves represent the SLRs. The horizontal red dashed lines indicate the energy of the electronic and vibronic transitions of the molecules, and gray solid curves illustrate the dispersions of the PEP.

not play a relevant role in the emission besides enhancing the out-coupling of light. Another salient feature of the emission, revealed with Fourier microscopy, is that this emission occurs in the full momentum space. In contrast to recent demonstrations of exciton-polariton lasing and condensation in organic systems [5,7–9], where the coherent emission above threshold has a defined wave vector, in our system there is not a mode at the emission frequency that defines the wave vector of the coherent emission. Instead, a speckle-like emission pattern due to structural imperfections is observed, modulated by the linear out-coupling of the emission by SLRs. This behavior of coherent emission arises from the presence of structural imperfections in the lattice, in contrast to the previously reported plasmon-exciton polariton (PEP) lasing in a defect-free lattice [7]. Interferometric measurements reveal the long-range spatial coherence over the pumped area, constituting a clear indication of the collective radiation of the molecules. These results demonstrate a novel and unconventional behavior of emission with enhanced spatial and temporal coherence in the nonlinear regime despite the absence of a well-defined emission momentum as could be expected from any exciton-polariton condensate or laser.

The scanning electron microscopy (SEM) image of the silver nanoparticle array is shown in Fig. 1(a). The long lattice constant (x direction) of the array is $a_1 = 380$ nm, and the short lattice constant is $a_2 = 200$ nm. The dimensions of the particles are $200\,\text{nm} \times 50\,\text{nm} \times 20\,\text{nm}$. A similar sample with a slightly longer lattice constant of $a_1 = 420$ nm has been fabricated with the same particle dimensions. The description of the sample fabrication is available in the Supplemental Material [17]. The array is covered with a 230-nm-thick layer of Poly(methyl methacrylate) doped with a rylene dye [N, N'-Bis(2,6-diisopropylphenyl)-1,7- and -1,6-Bis(2,6-diisopropylphenoxy)-perylene-3,4:9,10-tetracarboximide] with 45 wt% concentration of the dye in the polymer. The absorption and emission spectra of this dye are shown in Fig. 1(b). The two major peaks in the absorption spectrum at $E_{X_1} = 2.24$ eV and $E_{X_2} = 2.41$ eV correspond to the electronic transition and a vibronic transition of the molecules to the first excited state, respectively.

Arrays of plasmonic nanoparticles can support SLRs [18–21]. These are hybrid plasmonic-photonic modes resulting from the enhanced radiative coupling between localized surface plasmon resonances (LSPRs) of the individual nanoparticles through the in-plane orders of diffraction, i.e., Rayleigh anomalies (RAs). The dispersion of the RAs can be calculated using the grating equation describing the conservation of the in-plane momentum. A description of SLR dispersions is given in the Supplemental Material [17]. Strong field enhancement, along with a delocalized electric field, is characteristic of SLRs. These properties facilitate the interaction of SLRs with the organic molecules to achieve strong light-matter coupling and the formation of plasmon-exciton polaritons (PEPs) [22–25].

The angle-resolved extinction of the samples was measured using white light to determine the dispersion of the PEPs. A detailed description of the extinction measurements is given in the Supplemental Material [17]. The polarization of the incident light is fixed along the short axis of the nanoparticles (y axis) to excite the LSPRs along this axis. The samples were rotated around the x axis. In Figs. 1(c) and 1(d), we can see the extinction measurements of the arrays with $a_1 = 380$ nm and $a_1 = 420$ nm, respectively. These dispersions are similar for the two samples, albeit with an energetic redshift due to the longer lattice constant. The red dashed curves in this figure indicate the dispersion of the first-order SLR in a medium with an effective refractive index of 1.5. The nondispersive red dashed horizontal lines indicate the energies of the electronic transition and the first vibronic transition of the molecules. A clear anticrossing in the dispersion of the modes, characteristic of the strong light-matter interaction and the formation of PEPs, is seen at the energy and momentum where the SLR [$E_{\text{SLR}}(k)$] and molecular transition intersect. Considering only the coupling of the SLRs to the electronic transition (E_X), the upper- and lower-energy PEPs are given by $E^{\pm}(k) = \frac{1}{2}\left[E_{\text{SLR}}(k) + E_{\text{ex}} - i(\gamma_{\text{SLR}} + \gamma_X) \pm \sqrt{4g^2 + \left(E_{\text{SLR}}(k) - E_X - i(\gamma_{\text{SLR}} - \gamma_X)\right)^2}\right]$, where the Rabi energy $\hbar\Omega_R = 2g$ defines the coupling

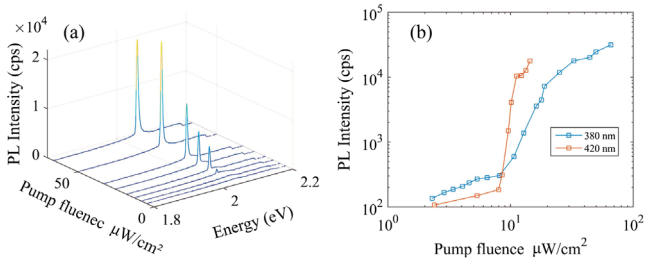

FIG. 2. (a) Emission spectra of the array of nanoparticles with lattice constant $a_1 = 380$ nm for different pump fluences. (b) Emission intensity at 2.032 eV as a function of the incident pump fluence for the arrays with lattice constants of 380 nm (blue) and 420 nm (red).

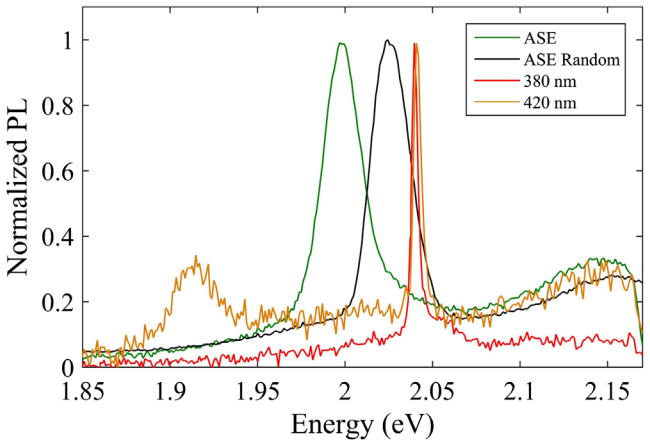

FIG. 3. ASE spectra of a PMMA layer with 45 wt% dye (green curve) and a similar layer on top of a array of random nanoparticles (black curve). The orange and red curves are the emission spectra of the arrays with lattice constants of 380 and 420 nm covered with PMMA/dye, pumped at $P = 1.2P_{\mathrm{th}}$. The peak at $E \approx 1.92$ eV corresponds to the emission of the lower PEP from a 420 nm pitch sample.

strength, and γ_{SLR} and γ_{X} are the decay rates of the SLR and the excitons, respectively.

The solid gray curves in Figs. 1(c) and 1(d) correspond to the dispersion of the coupled states obtained by diagonalization of the Hamiltonian in which the coupling of the molecular transitions to the SLR are considered, but neglecting the coupling between the electronic transition and the vibronic transition (see the Supplemental Material [17]). A Rabi energy splitting of 220 meV is obtained between the lower and middle polariton bands.

To study the emission properties of the samples at different pump fluences, they were pumped using pulses of 100 fs and $E_{\mathrm{pump}} = 2.455$ eV under normal incidence. The repetition rate of the pump laser was 1 kHz. The emission from the sample was collected along the normal direction. In Fig. 2(a), the emission of the sample with $a_1 = 380$ nm is shown as a function of the photon energy and pump fluence. By increasing the pump laser intensity, the emission intensity increases linearly until the emergence of the threshold and the nonlinear increase of the emission intensity. The sample with $a_1 = 420$ nm manifests a similar behavior (see Fig. S1 in the Supplemental Material [17]). To illustrate the nonlinear behavior of the emission of both samples, the emission intensity at the forward direction is plotted as a function of the incident pump fluence in Fig. 2(b). Polarization-dependent measurements displayed in Figs. S3 and S4 in the Supplemental Material show that the emission is mainly polarized along the y axis [17].

To fully characterize the emission properties of the dye molecules, we have implemented two separate control experiments. In the first experiment, we measured the amplified spontaneous emission (ASE) of a 230-nm-thick layer of PMMA doped with 45 wt% dye molecules in the absence of any plasmonic structure. The spectrum of the ASE is shown in Fig. 3 as a green curve. Furthermore, to illustrate the effect of the periodic structure and SLRs on the formation of the PEPs and to exclude the possibility of plasmonic lasing (spaser) through LSPRs, we have fabricated an array of random nanoparticles with the same size and geometry of the nanoparticles of the periodic arrays and covered it with an identical dye-doped polymer layer. By pumping the random array, we do not observe lasing even at the highest fluences reachable by our laser. The main difference with the bare molecular layer is that the broad peak of the ASE is slightly blueshifted due to the interplay of the loss and gain in the presence of the plasmonic nanoparticles.

The vibrational quantum of the molecules in our system has an energy $E_{\mathrm{X}_1} - E_{\mathrm{X}_2}$, i.e., the energy difference between the electronic transition and the first vibronic transition in the absorption spectrum. The role of vibronic relaxation on the nonlinear emission energy is shown in Fig. 3, where the emission spectra above the threshold ($P = 1.2P_{\mathrm{th}}$) for samples with the pitch sizes of 380 and 420 nm are plotted. It can be seen that the energy of the nonlinear emission peak is insensitive to the significant change in the lattice constant and the dispersion of the SLRs. These measurements confirm that the emission frequency is independent of the cavity frequency and is locked one vibrational quantum below the exciton-polariton reservoir (the zero-phonon line of the molecules). In this case, the effect of the cavity is limited to strongly coupling the optical mode to the molecular excitons. The radiative scattering of PEPs with molecular vibronic states leads to the coherent emission.

Having established the role of vibronic relaxation in the nonlinear regime, we can wonder about the effect that this molecular process has in the momentum distribution of the emission. For organic-based exciton polaritons in which the molecules are randomly distributed in the polymer matrix, the relaxation of exciton polaritons occurs due to the scattering from the vibrations localized

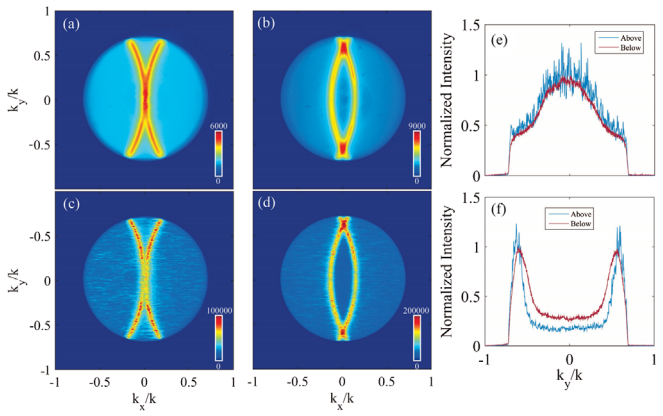

FIG. 4. Fourier image of the emission below the threshold ($0.8P_{\mathrm{th}}$) from the samples with lattice constants of (a) 380 nm and (b) 420 nm along the x direction. Fourier image of the emission from the samples beyond the threshold ($1.2P_{\mathrm{th}}$) from the samples with lattice constants of (c) 380 nm and (d) 420 nm. (Unit of intensity is cps.) Cross section of the Fourier pattern below and above the threshold at $k_x/k = 0$ and along k_y/k for lattice constants of (e) 380 nm and (f) 420 nm.

on the individual molecules collectively coupled to the optical mode, i.e., the SLR. The momentum of exciton polaritons after vibronic relaxation with phonons is not well defined due to the localization of this process on individual molecules. Consequently, we should expect a broad momentum distribution of emitted photons after relaxation [13]. Hence, unlike inorganic exciton polaritons, the momentum is not necessarily a good quantum number to describe the nonlinear emission. The distribution of momenta after the scattering of PEPs from molecular vibrations can be determined by measuring the angular distribution of the emitted photons. Measuring the intensity at the back focal plane of the objective lens used to collect the emission is a straightforward method to access this information. We have used a 50× objective with a $NA = 0.6$ to collect the emission. In these measurements, the pumped area is kept larger than the field of view of the objective. The Fourier patterns of the emission from the samples with $a_1 = 380$ and 420 nm are shown in Figs. 4(a,b) at a pump fluence below the threshold ($P = 0.8P_{\mathrm{th}}$), and using a bandpass filter at $E = 2.032 \pm 0.016$ eV to collect solely the nonlinear emission above the threshold. The emission patterns of both samples at pump fluences below the threshold are the result of the enhanced out-coupling due to the lattice [26].

Figures 4(c) and 4(d) show the Fourier patterns obtained from the samples by pumping above the threshold. Even above the threshold, the emission is not limited to specific wave vectors as previously reported in similar hole arrays or nanoparticle arrays weakly and strongly coupled to organic molecules [7,27–29]. This remarkable behavior is clearly seen in the measurements of the emission above threshold taken by rotating a detector around the sample, as

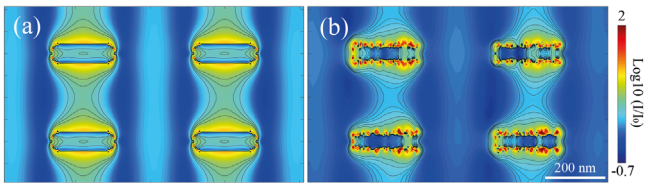

FIG. 5. FDTD simulations of the electric-field intensity for the 380 nm pitch size sample (a) without and (b) with imperfections.

shown in Fig. S5 in the Supplemental Material [17]. Instead of a well-defined wave vector for the nonlinear emission, this emission is omnidirectional, with a speckle pattern in reciprocal space. The speckle pattern can be attributed to the fact that the detected emission is the result of the localized coherent emissions and the interference in the far field. In addition, the PEP bands are also visible in the Fourier patterns above threshold. Similar to the emission enhancement below threshold, at these bands the intensity is enhanced by the out-coupling of the emission. We have confirmed that the PEP bands do not play a major role in defining the momentum of the nonlinear emission by measuring it both below and above threshold, and regardless of the pump fluence, the ratio of the intensity emitted along the PEPs bands with respect to the intensity emitted in different directions remains nearly constant. These measurements are shown in Figs. 4(e) and 4(f), where the normalized intensity profiles to the averaged maximum of the emission below and above threshold along k_y/k are displayed. This constant intensity ratio confirms that the optical modes contribute to the enhancement of the out-coupling of the emission, but not in the nonlinear emission process itself. We note that the absence of a defined emission momentum despite the large temporal coherence is one of the major differences with respect to the conventional band-edge lasing or exciton-polariton lasing from plasmonic systems where the emission occurs in a well-defined direction [7,27–30]. This characteristic of the coherent emission supports the argument that the emission from strongly coupled molecules to SLRs originates from local (molecular) sources with undefined momentum [13]. In particular, we need to take into account the role of disorder and imperfections in the nanostructure during the fabrication process [31]. Due to the imperfections in the lattice or within the polymer matrix, localized electric-field hot spots can be formed that lead to flat dispersion of the emission (see Fig. S6 in the Supplemental Material [17]). To gain insight into the modification of the electric fields due to the presence of imperfections, we have simulated the electric-field intensity in the array of silver nanoparticles at the frequency of the SLR in both the absence and presence of imperfections (see the Supplemental Material for details [17]). In the absence of imperfection [Fig. 5(a)], the electric fields are more homogeneously distributed over the space, and significant radiative coupling between the particles is visible due to the collective nature of SLRs. By introducing

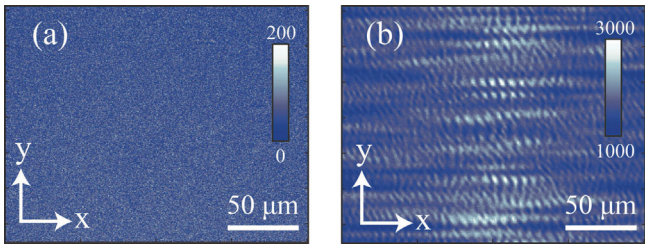

FIG. 6. Interference pattern of the emission from the sample (a) below ($P = 0.6P_{th}$) and (b) above threshold ($P = 1.5P_{th}$) for a sample with the pitch size of 420 nm. A bandpass filter at $E = 2.032 \pm 0.016$ eV is used to select the nonlinear emission.

the imperfections in the array [Fig. 5(b)], many near-field hot spots can be observed besides a less pronounced long-range radiative coupling between the nanoparticles. To better illustrate the role of disorder on the nonlinear behavior, we have included the Fourier space measurements of the sample studied previously in Ref. [7] in the Supplemental Material (Figs. S8 and S9) [17]. These comparisons illustrate the very different emission properties in samples with different degrees of disorder. The larger imperfections in the current sample prevent the system from radiating with a well-defined momentum, i.e., a general property of polariton lasing.

An interesting observation is the long-range spatial coherence of the nonlinear emission, despite its localized nature. Long-range spatial coherence in the samples was measured using a Michelson interferometer, where in one of the arms a retroreflector is placed to make a centrosymmetric image of the original emission image. The images of the two arms of the interferometer are overlapped on a CCD camera. No interference fringes are visible in any of the samples when they are pumped below the nonlinear threshold [see Fig. 6(a)], indicating the absence of coherence in the linear regime. In contrast, fringes over the full image appear in the interferogram when the pump fluence is increased above threshold [see Fig. 6(b)]. These fringes indicate the persistence of long-range spatial coherence, although the emission is originated from localized sites, which points toward the role of radiative coupling between the nanoparticles leading to the formation of SLRs.

In conclusion, we have shown a new emission regime of organic molecules coupled to collective plasmonic resonances. In particular, we have demonstrated that an ensemble of excited molecules with an electronic transition strongly coupled to a surface lattice resonance in an array of plasmonic nanoparticles radiates coherently despite the presence of structural imperfections. In contrast to organic polariton condensates, where there is a well-defined emission momentum, the nonlinear emission in our study is not significantly influenced by the optical modes, and a speckle-like pattern is measured in all the probed directions. The frequency of the emission is solely determined by the vibrational quanta of the individual molecules. We also measure a long-range spatial coherence, confirming the coherent emission of the strongly coupled molecules.

This research is supported by the Netherlands Organisation for Scientific Research (NWO) through the Industrial Partnership Program Nanophotonics for Solid State Lighting between Philips and NWO.

*Corresponding author.
j.gomez.rivas@tue.nl

[1] H. Deng, H. Haug, and Y. Yamamoto, Rev. Mod. Phys. **82**, 1489 (2010).
[2] J. Bellessa, C. Bonnand, J. C. Plenet, and J. Mugnier, Phys. Rev. Lett. **93**, 036404 (2004).
[3] J. Dintinger, S. Klein, F. Bustos, W. L. Barnes, and T. W. Ebbesen, Phys. Rev. B **71**, 035424 (2005).
[4] J. del Pino, F. J. Garcia-Vidal, and J. Feist, Phys. Rev. Lett. **117**, 277401 (2016).
[5] S. Kéna-Cohen and S. R. Forrest, Nat. Photonics **4**, 371 (2010).
[6] S. Zaster, E. R. Bittner, and A. Piryatinski, J. Phys. Chem. A **120**, 3109 (2016).
[7] M. Ramezani, A. Halpin, A. I. Fernández-Domínguez, J. Feist, S. R. -K. Rodriguez, F. J. Garcia-Vidal, and J. G. Rivas, Optica **4**, 31 (2017).
[8] J. D. Plumhof, T. Stöferle, L. Mai, U. Scherf, and R. F. Mahrt, Nat. Mater. **13**, 247 (2014).
[9] K. S. Daskalakis, S. A. Maier, R. Murray, and S. Kéna-Cohen, Nat. Mater. **13**, 271 (2014).
[10] T. Cookson, K. Georgiou, A. Zasedatelev, R. T. Grant, T. Virgili, M. Cavazzini, F. Galeotti, C. Clark, N. G. Berloff, D. G. Lidzey, and P. G. Lagoudakis, Adv. Opt. Mater. **5**, 1700203 (2017).
[11] G. Lerario, A. Fieramosca, F. Barachati, D. Ballarini, K. S. Daskalakis, L. Dominici, M. De Giorgi, S. A. Maier, G. Gigli, S. Kéena-Cohen, and D. Sanvitto, Nat. Phys. **13**, 837 (2017).
[12] D. Sanvitto and S. Kéna-Cohen, Nat. Mater. **15**, 1061 (2016).
[13] L. Mazza, L. Fontanesi, and G. C. La Rocca, Phys. Rev. B **80**, 235314 (2009).
[14] N. Somaschi, L. Mouchliadis, D. Coles, I. E. Perakis, D. G. Lidzey, P. G. Lagoudakis, and P. G. Savvidis, Appl. Phys. Lett. **99**, 143303 (2011).
[15] J. A. Ćwik, S. Reja, P. B. Littlewood, and J. Keeling, Europhys. Lett. **105**, 47009 (2014).
[16] M. Slootsky, Y. Zhang, and S. R. Forrest, Phys. Rev. B **86**, 045312 (2012).
[17] See Supplemental Material at http://link.aps.org/supplemental/10.1103/PhysRevLett.121.243904 for more information about methods of experiment, measurements related to the polarization of the emission, angle-resolved photoluminescence and extended description about the simulations of the disordered structures.
[18] S. Zou, N. Janel, and G. C. Schatz, J. Chem. Phys. **120**, 10871 (2004).
[19] G. Vecchi, V. Giannini, and J. Gómez Rivas, Phys. Rev. Lett. **102**, 146807 (2009).
[20] A. D. Humphrey and W. L. Barnes, Phys. Rev. B **90**, 075404 (2014).

[21] R. Guo, T. K. Hakala, and P. Törmä, Phys. Rev. B **95**, 155423 (2017).
[22] S. Rodriguez and J. G. Rivas, Opt. Express **21**, 27411 (2013).
[23] A. I. Väkeväinen, R. J. Moerland, H. T. Rekola, A. P. Eskelinen, J. P. Martikainen, D. H. Kim, and P. Törmä, Nano Lett. **14**, 1721 (2014).
[24] F. Todisco, M. Esposito, S. Panaro, M. De Giorgi, L. Dominici, D. Ballarini, A. I. Fernández-Domínguez, V. Tasco, M. Cuscun, A. Passaseo, C. Cirac, G. Gigli, and D. Sanvitto, ACS Nano **10**, 11360 (2016).
[25] M. Ramezani, A. Halpin, J. Feist, N. Van Hoof, A. I. Fernández-Domínguez, F. J. Garcia-Vidal, and J. Gomez Rivas, ACS Photonics **5**, 233 (2018).
[26] G. Lozano, G. Grzela, M. A. Verschuuren, M. Ramezani, and J. Gomez Rivas, Nanoscale **6**, 9223 (2014).
[27] F. van Beijnum, P. J. van Veldhoven, E. J. Geluk, M. J. A. de Dood, G. W. 't Hooft, and M. van Exter, Phys. Rev. Lett. **110**, 206802 (2013).
[28] W. Zhou, M. Dridi, J. Y. Suh, C. H. Kim, D. T. Co, M. R. Wasielewski, G. C. Schatz, and T. W. Odom, Nat. Nanotechnol. **8**, 506 (2013).
[29] A. H. Schokker and A. F. Koenderink, Phys. Rev. B **90**, 155452 (2014).
[30] A. H. Schokker and A. F. Koenderink, Optica **3**, 686 (2016).
[31] V. Savona, J. Phys. Condens. Matter **19**, 295208 (2007).